

RESEARCH PAPER

EVALUATION OF THE INFLUENCE OF WASTE GLASS POWDER (WGP) ON THE THERMO-MECHANICAL PERFORMANCE OF FIRED CERAMICS

Abayomi Adewale Akinwande¹, Adeolu Adesoji Adediran^{2*}, Oluwatosin Abiodun Balogun¹, Oladele Bello¹, Abel Barnabas¹, Oluwayomi Peter Balogun¹, Olanrewaju Seun Adesina²

¹Department of Metallurgical and Materials Engineering, Federal University of Technology Akure, P.M.B. 704, Ondo State, Nigeria.

²Department of Mechanical Engineering, Landmark University, Omu- Aran, PMB 1001, Kwara State, Nigeria.

*Corresponding author: dladesoji@gmail.com, abypublications@gmail.com, tel.: 2348162542747, Department of Mechanical Engineering, Landmark University, Omu-Aran, PMB 1001, Kwara State, Nigeria.

Received: 30.04.2020

Accepted: 11.07.2020

ABSTRACT

Effects of elevated temperature on thermo-mechanical properties of fired ceramic products reinforced with waste glass powder (WGP) were reported. Samples were produced by the addition of WGP to clay in varied amount and oven dried samples were fired in an electric furnace which was operated 1200 °C. Compressive and flexural strength were examined at room temperature and at elevated temperatures of 100, 300, 500, 700, and 900 °C. Results showed that, compressive strength and flexural strength reduced at elevated temperatures. Thermal conductivity, diffusivity, and emissivity were higher with increasing WGP content, while thermal expansivity and specific heat capacity were lower as percentage WGP increased in the samples. Results on thermal shock resistance showed that WGP reduced shock resistance in the samples, while the cooling rate increased with the percentage addition of WGP. Impact resistance was noted to decrease in samples when fast cooled from high temperature as the rapid cooling rate was observed to increase with WGP addition in samples. It was concluded that for fired clay products incorporated with WGP, the operating temperature should not exceed 700 °C. Also, in an environment whereby cooling is done by air or/and water, an operating temperature of ≤ 300 °C was recommended.

Keywords: clay, flexural, compressive, emissivity, waste glass powder,

INTRODUCTION

Fired clay is a kind of ceramic material made from moulded clay by the process of heat in order to make it hard and strong. It has good resistance to high temperature, having a fusion point higher than 1600 °C and is corrosion resistant [1,2]. Fired clay materials are used for lining of furnaces as fired bricks and for industrial production of white wares and other products. Some fired bricks are employed in masonry for housing and for roof tiles application [3]. Properties of fired clay products include porosity, high temperature resistance, wear resistance, and high compression. These properties can vary with temperature, which birth the study of the behaviour of fired bricks under different temperature conditions. This study considered thermo-mechanical behaviour of fired clay samples at different thermal conditions because performance of ceramic materials tends to change at elevated temperature. Studies on thermal behaviour of fired ceramics may reveal how additives affect thermal and mechanical behaviour of fired clay bricks and possibly provide information on possible application of such products. In previous study, [4] observed increased bulk and true density as eggshell increased in fired bricks. For water absorption, the value reduced with increasing egg shell content. Coefficient of thermal expansion was noticed to reduce in the samples. At 20 wt. % eggshell addition, compressive strength, and hardness were highest at 8.28 MPa and 8.79 HV respectively while thermal expansion coefficient was lowest at $2.3652 \times 10^{-6}/K$.

In another report on thermal behaviour of insulating brick developed using saw dust additive [5], ball clay and kaolin used were sieved to 0- 45 μ m, 45-53 μ m, 63-90 μ m, 90 – 125 μ m and 125-154 μ m. The saw dust was sieved to 0-125 μ m, 125-154 μ m, 154-180 μ m and 355-425 μ m and was added to the mixture of ball clay and kaolin. Results obtained showed that density and thermal conductivity reduced as particle sizes of kaolin and ball clay increased for different sizes of saw dust considered. Specific heat capacity increased while coefficient of thermal diffusivity reduced as particle sizes of kaolin and clay increased. The effect of coal and wheat husk addition on thermal properties of clay bricks was reported by [6]. From their work, it was observed that thermal conductivity reduced as percentage coal and wheat husk increased from 0 to 50 wt. %. Wheat husk was more effective in improving insulation properties of the clay bricks compared to charcoal due to increased pores formed. Also, it gave reduction of up to 92 % in

thermal conductivity. Thermal diffusivity was shown to reduce with increased additives and decrease between 15 and 60 % for charcoal additives of 5 to 50 wt. % while that of wheat husk was 44 to 92 %. Mechanical strength was noted to decrease with increase in water absorption, apparent porosity, and firing shrinkage. Wheat was more effective for insulation than charcoal.

MATERIAL AND PREPARATION PROCEDURE

Clay was obtained from a borrow pit in Awule community, Akure (latitude 7.250771 °, longitude 5.210266 °) in Ondo state, Nigeria by excavation using a shovel and collected into a container. Waste glass bottles which were obtained from a local waste glass seller, were employed in this study. The clay was treated by mixing with water in a container and allowed to settle for 2 days, after which the suspended water was poured away. The clay was further treated by adding fresh water, stirring and allowing settling for another 2 days. The suspended water was poured away and the left over clay was spread in open atmosphere to sundry for 3 days. Dried clay was crushed, milled (using modified ball mill, serial number F-N 178) and sieved to -150 μ m before been packed into a container. Similar protocol was obtained with waste glass using an electric sieve shaker. Waste glass powder (WGP) and clay powder sieved to -150 μ m were collected, separated, and used in sample preparation.

The clay and waste glass powder were thoroughly mixed in an electric mixer in varying amount. WGP was added to clay in the proportion of 0 to 40 wt. % at 5 wt. % interval. Water was added to clay in the ratio of 1:3 and mixed thoroughly. The slurry obtained was compressed (at 10 MPa) into cylindrical moulds of diameter 50 mm, height 100 mm and diameter 40 mm and height 20 mm, rectangular moulds of dimensions 150 mm \times 150 mm \times 150 mm, 400 mm \times 100 mm \times 100 mm and 190 mm \times 90 mm \times 90 mm. Green bricks produced which initially were left in open air for 24 hours for stability were oven dried for 12 hours at 110 °C after which they were fired in an electric furnace at 5 °C/min until 1200 °C was attained. The samples were soaked for 2 hours at that temperature before been allowed to cool to room temperature and taken out for examination.



Fig. 1 Pictures of (a) electric furnace used in firing and (b) bricks samples

TEST PROCEDURE

Mechanical properties

Mechanical properties were studied by initially carrying out compressive strength (for rectangular samples of dimension 150 x 150 x 150 mm) and flexural strength (for rectangular samples of dimension 400 x 100 x 100 mm) test on brick samples at 26–29 °C (room temperature). Effect of heat on mechanical properties of samples were evaluated by heating to 100, 300, 500, 700, 900, and 1000 °C, soaked for 1 hour and tested for compressive strength and flexural strength immediately they were brought out from the furnace. The test was carried out in line with [7] for compressive strength and [8] for flexural strength. Percentage reduction in strength ($\Delta\%$) was evaluated using Equation (1) for that of compressive strength and Equation (2) for flexural strength. Flexural strain at fracture (for different temperatures) was evaluated using Equation (3).

$$\Delta C\% = \frac{C_n - C_i}{C_i} \quad (1)$$

$$\Delta F\% = \frac{F_n - F_i}{F_i} \quad (2)$$

$$\text{Flexural strain } (\alpha) = \frac{6dt}{h^2} \quad (3)$$

Where, $\Delta C\%$ is percentage reduction in compressive strength,
 $\Delta F\%$ is percentage reduction in flexural strength,
 F_i/C_i is Flexural/compressive strength at initial temperature,
 F_n/C_n is Flexural/compressive strength at new/next temperature,
 d is the recorded deflection (mm) at different temperatures,
 t is thickness of sample and
 h is the distance between two supports.

Resistance to impact was examined by applying a load rate of 5 N/min at the centre of the brick samples from a height of 50 cm until fracture occurred. The number of cycle was recorded for each sample at room temperature (26 – 29 °C) and at temperatures of 100, 300, 500, 700, 900, and 1000 °C.

Thermal properties

Cylindrical samples of diameter 40 mm and height 20 mm were tested for thermal conductivity using hot plate method in line with [9], linear and volumetric thermal expansion were evaluated in line with [10] by measuring the dimension of each brick sample at various temperature and evaluated using Equation (4) and (5). Specific heat capacity was accessed by method of mixture using cylindrical samples of diameter 50 mm and height 100 mm [11] while thermal emissivity was examined in line with [12] and thermal diffusivity [13] was calculated using Equation (6).

$$\text{Linear expansion} = \frac{L_2 - L_1}{L_1 \Delta T} \quad (4)$$

$$\text{Volumetric expansion} = \frac{V_2 - V_1}{V_1 \Delta T} \quad (5)$$

$$\text{Thermal diffusivity} = \frac{k}{\gamma C_p} \quad (6)$$

Where L_1 is initial length at previous temperature (m),
 L_2 is final length at new temperature (m),
 V_1 is initial volume at previous temperature (m^3),
 V_2 is final volume at new temperature (m^3),
 ΔT is temperature difference (K),
 K is thermal conductivity,
 γ is density and
 C_p is specific heat capacity.

Thermal shock resistance and cooling rate

Thermal shock resistance was determined by three experimental procedures, while cooling rate was evaluated at normalized cooling and rapid cooling:

- I. Exp. 1: rectangular bricks samples were heated to 1000 °C at 5 °C/min and soaked for 1 hour and then held in air for 10 mins. The process was continued until crack occurred and the number of cycles was recorded in line with [14].
- II. Exp. 2: heating samples to 300 °C at 5 °C/min, soaking for 1 hour and holding the samples in open air. Air was blown on the samples at room temperature at rate of 12.2 cm^3/s for 10 minutes. The procedure was followed until crack occurred and the number of cycles recorded.
- III. Exp. 3: heating samples to 300 °C at 5 °C/min, soaking for 1 hour and holding the samples in open air and allowing drip of water 8.38 cm^3/s for 10 mins. The process continued until crack appeared and the number of cycles recorded.
- IV. Normalized Cooling rates of samples was evaluated by heating samples to 300, 500, 700, and 900 °C at 5 °C/min held for 30 mins and allowed to cool to room temperature in air. Cooling time to room temperature was observed, the cooling rate was evaluated using Equation (7).
- V. Fast cooling rate was measured by heating samples to 300, 500, 700, and 900 °C at 5 °C/min, held for 30 mins and cooled to room temperature (26 °C) by applying water at a fast rate (fast cooling rate) of 16.8 cm^3/s on the samples. The time taken was recorded and cooling rate was evaluated using Equation (7). Cooling rate coefficient was obtained as ratio of normalized cooling rate to high cooling rate.

$$\text{Cooling rate} = \frac{T_2 - T_1}{A \times t} \quad (7)$$

T_2 is final temperature,
 T_1 is initial temperature,
 A is cross sectional area of sample and
 t , time taken to cool.

RESULTS AND DISCUSSION

Morphological representation of some samples at room temperature (26 °C)

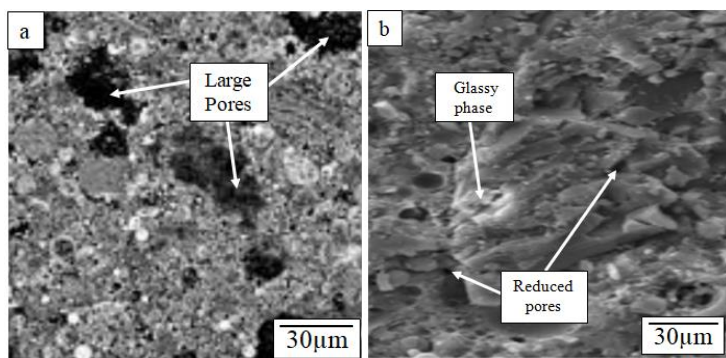


Fig. 2 SEM image samples at (a) 0 wt. % WGP (b) 30 wt. % WGP at room temperature

Figure 2 (a) shows the SEM image of brick sample with 0 % WGP addition at room temperature of 26 °C. Pores are observed in 0 wt. % sample, when compared with bricks containing 30 wt. % WGP which had reduced pores. This explains reason for lower compressive and flexural strength in sample with 0 % WGP when compared with that of 30 wt. % WGP. Figure 2b shows image of 30 wt. % WGP addition, porosity reduced and the presence of glass luster as a result of glassy phase formed at high temperature was evident. The bond between WGP, clay particles and the strong glassy phase formed in samples resulted into improved strength compared to the one of 0 wt. % WGP as reported in Table 1.

Thermo-Mechanical properties at room temperature

a. Mechanical strength at room temperature

Table 1 Compressive and Flexural strength at room temperature (26 °C)

%WGP	0	5	10	15	20	25	30	35	40
CS	7.4	8.2	9.7	11.3	13.3	13.7	14.5	12.1	11.3
FS	1.05	1.24	1.47	1.79	2.50	2.61	2.63	2.31	2.17
RS	12	12	13	15	18	16	16	14	12
FSt(x 10⁻³)	11	8.1	6.3	4.1	3.3	1.8	0.9	0.6	0.4

CS represents compressive strength (MPa), FS represents Flexural strength (MPa), RS represents resistance to impact (number of cycles) and FSt represents flexural strain (mm/mm).

As WGP increased in proportion, mechanical strength increased (Figure 3). WGP particles filled up the pores in the clay matrix, thereby reducing porosity. As temperature increased during firing, dehydration increased, compactment and stabilization were also enhanced at temperatures between 20 to 600 °C. As the temperature was being raised, chemical reaction occurred leading to fusion of the clay and WGP particles, which resulted in enhanced strength and hardness in the samples [15][16]. At above 900 °C, vitrification occurred leading to formation of glassy phase [17] which proportion is dependent on the proportion of WGP added. The glassy phase formed further covered the pores leading to reduction in porosity and enhanced compactment as confirmed in [18]. The consequent result is increased strength and hardness. Care was taken not to fire above 1200 °C due to possibility of expansion of the glassy phase so as not to allow crack or storage of residual stress. However, glassy phase is brittle; hence, addition of WGP particles to a certain extent may result in decrease in strength which explains the reduction of compressive and flexural strength at 35 and 40 wt. % additions (Table 1). Resistance to impact increased from 0 wt. % to 20 wt. % and reduced further as WGP content increased due to increased glassy phase. The results reported in this study are in line with [19][20], where increase in strength was observed with increasing waste glass addition. Flexural strain reduced continuously from 0 wt. % to 40 wt. % of WGP as indicated in Table 1.

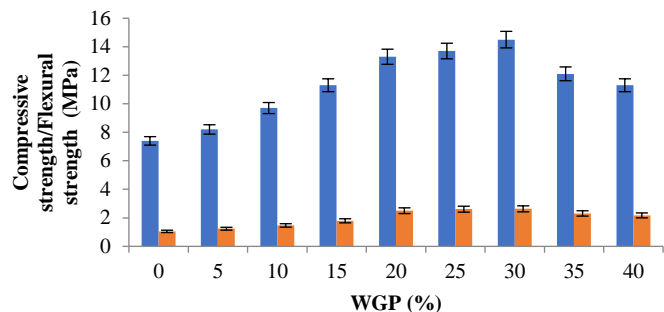


Fig. 3 Variation in compressive/flexural strength at increasing WGP proportion

Thermal properties

a. Thermal conductivity

With increasing waste glass powder (WGP) content, thermal conductivity was rising (Figure 4) which is attributed to reduction in porosity. These pores serve as air trap and reduce thermal transfer since air has poor thermal conductivity. This is backed up with the fact that presence of WGP causes lower volume of pores since the pores are filled with glass powder particles, hence resulting in increased thermal conductivity. The observation is also linked to interlocking of particle of the waste glass powder and clay within the structure because of well graded particle size distribution [5].

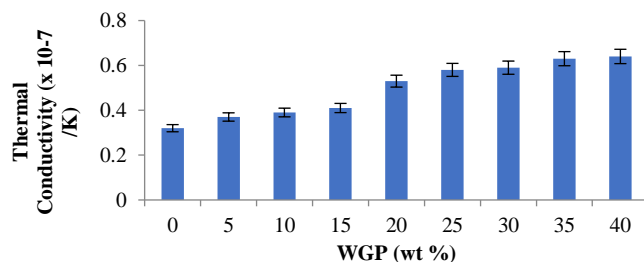


Fig. 4 Effects of WGP on thermal conductivity

Coupled with this, is reduced interparticle distance resulting in low porosity, leading to high bond strength which enhanced thermal movement within the solid clay body. The phenomenon led to high internal vibration of particles when the body was thermally activated thereby resulting in increased transfer of thermal energy from one particle to another. Pore formers has been known to increase pores in bricks leading to reduction in thermal conductivity as reported in [5][21][22] which is due to the fact that the pores serve as air trap and since air is poor conductor, this leads to decrease in thermal conductivity. On the other hand, addition of waste glass in fired bricks results in reduction in porosity which eventually amount to increase in thermal conductivity as observed in this study

b. Thermal diffusivity and emissivity

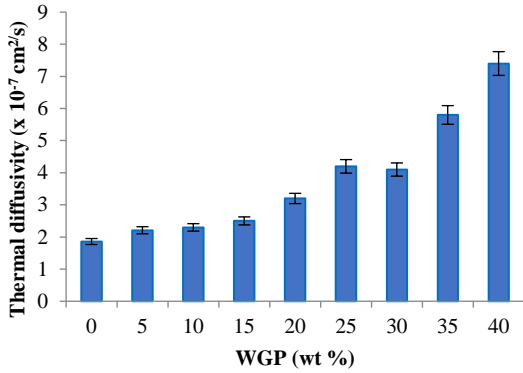


Fig. 5a Effect of WGP content on thermal diffusivity

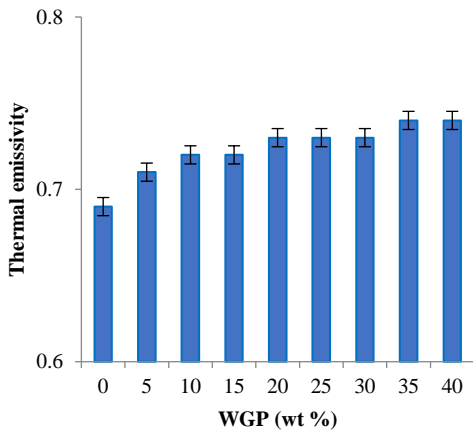


Fig. 5b Effect of WGP content on thermal emissivity

Thermal diffusivity refers to rate at which heat is transferred from the hot end of a material to the cold end of such material [23], while emissivity refers to the ability of a body to emit thermal radiation at the surface [24]. Diffusivity which was evaluated at 300 °C was observed to be higher with additional WGP content (Figure 5a). This occurred due to reduced porosity leading to shorter interparticle distance and stronger bond between particles, which enabled easy transmission and diffusion of heat within particles. Emissivity increased gradually as WGP increased up to 20 wt. % WGP remained constant up to 35 and 40 wt. % of WGP after which there was progressive rise up to 40 wt. % (Figure 5b). High absorptivity of heat may result into higher emissivity due to lower capacity to retain heat as interparticle distance reduced. Increased porosity results into lower diffusivity as reported in [6]. In this study, the results showed increment in diffusivity due to lower porosity.

c. Specific heat capacity

Specific heat capacity is the “amount of heat needed to raise the temperature of a unit mass of a material by 1K” [25]. The higher the value, the higher the amount of heat energy required to raise the temperature of a unit mass of the object by 1K. Porous materials require much higher energy to raise temperature and in insulating bricks, these pores are filled with air which has poor conducting properties.

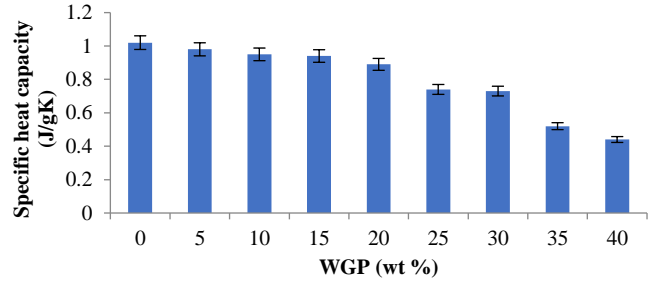


Fig. 6 Effect of WGP content on specific heat capacity

As the pores reduced and particles bond became stronger, the heat energy requirement became lower. This explains reason for the reduction in specific heat capacity as WGP increased (Figure 6). Increase in porosity reduces interparticle distance, hence, requires higher energy to raise the temperature of unit mass by 1K as reported in [5]. Reduction in porosity on the hand, led to shorter interparticle distance, thereby enhancing cohesion. Therefore, decrease in specific heat capacity with higher content of the additive was observed in this study (Figure 6) contrary to the outcome in [5].

Thermo-Mechanical performance at elevated temperature

a. Effects of increased temperature on compressive strength.

Table 2 Percentage reduction in compressive strength at different temperature for WGP-bricks

%WGP content in samples	Compressive strength at 26 °C	Percentage reduction in compressive strength (ΔC%)					
		100 °C	300 °C	500 °C	700 °C	900 °C	1000 °C
0	7.4	2.8	4.6	6.9	8.9	17.3	22.5
5	8.2	2.3	4.1	6.8	8.1	16.5	20.6
10	9.7	1.2	4.3	6.6	7.7	15.3	19.3
15	11.3	0.9	3.7	5.5	6.9	13.8	18.4
20	13.3	0.8	3.5	5.2	7.6	13.5	16.8
25	13.7	0.6	3.5	4.9	4.7	12.5	15.9
30	14.5	0.6	3.4	4.3	4.2	10.5	11.6
35	12.1	0.6	3.7	4.3	5.1	16.0	14.4
40	11.3	0.6	3.5	6.7	5.3	14.8	18.7

At elevated temperature (Table 2 and Figure 7), compressive strength depreciated due to gradual weakening of the bond between clay particles as well as reduction in adhesion between WGP particles and clay particles. As WGP increased in the samples, the value of ΔC% reduced, due to enhanced strength of adhesion between particles as WGP increased in the samples. Going from 100 °C to 700 °C for 0 to 40 wt. % WGP, percentage reduction in compressive strength increased gradually, for each WGP content ranging from 2.8 % to 8.9 % for 0 % WG, 2.3 to 8.1 % for 5 wt. % WGP, 1.2 to 7.7 % for 10 wt. % of WGP, 0.9 to 6.9 % for 15 wt. % of WGP, 0.8 to 7.6 % for 20 wt. % WGP, 0.6 to 4.7 % for 25 wt. % WGP, 0.6 to 4.2 % for 30 wt. % WGP, 0.6 to 5.1 % for 35 wt. % WGP and 0.6 to 5.3 % for 40 wt. % WGP. It was observed that at 100 °C, ΔC% value remained constant at 25 to 40 wt. % WGP content of 0.6 %.

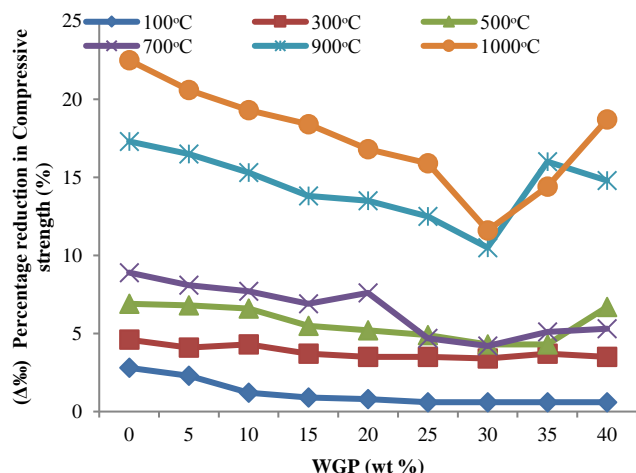


Fig. 7 Percentage reduction in compressive strength at increased temperature

On each temperature of 100 to 700 °C, ΔC% value reduced as WGP content increased. From 700 to 900 °C for each sample, ΔC% value reduced drastically from 8.9 to 17.3 % for 0 wt. % WGP, 8.1 to 16.5 % for 5 wt. % WGP, 7.7 % to 15.3 % for 10 wt. % WGP, 6.9 to 13.8 % for 15 wt. % WGP, 7.6 to 13.5 % for 20 wt. % WGP, 4.7 to 12.5 % for 25 wt. % WGP, 4.2 to 10.5 % for 30 wt. % WGP, 5.1 to 16 % for 35 wt. % WGP and 5.3 to 14.8 % for 40 wt. % WGP. At 1000 °C, ΔC% further fell to 22.5 %, 20.6 %, 19.3 %, 18.4 %, 16.8 %, 15.9 %, 11.6 %, 14.4 % and 18.7 % for 0, 5, 10, 15, 20, 25, 30, 35 and 40 WGP content respectively. The decrease for each of the mix proportion at 900 and 1000 °C is above 10 %, indicating that at temperature up to 900 °C, there was drastic weakening of the bond and degradation of the glass phase present, therefore, the working temperature of this clay samples under consideration is ≤ 700 °C. It was further observed that there was a measure of stability for samples with 25 and 30 wt. % addition of WGP which ΔC% values between 100 and 700 °C were less than 5 %, showing that WGP of 25 and 30 wt. %, will be most stable when operation temperature is ≤ 700 °C, beyond that, there could be degradation and drastic depreciation in strength.

b. Effects of increased temperature on flexural strength

Table 3 Percentage reduction in flexural strength at different temperatures

% WGP content in samples	Flexural strength at 26 °C	Percentage reduction in flexural strength (ΔF %) °C					
		100 °C	300 °C	500 °C	700 °C	900 °C	1000 °C
0	1.05	2.4	3.9	4.7	3.9	12.5	17.3
5	1.24	2.1	3.4	3.9	4.2	11.7	15.8
10	1.47	0.9	2.5	3.4	3.5	11.4	13.6
15	1.79	0.8	2.1	3.3	3.5	9.8	12.8
20	2.50	0.6	2.1	2.9	3.1	7.2	10.2
25	2.61	0.5	1.9	2.4	2.9	6.8	9.8
30	2.63	0.4	1.7	2.1	2.3	6.3	9.7
35	2.31	0.3	1.2	2.3	2.5	6.4	9.9
40	2.17	0.3	0.8	2.1	2.8	8.8	10.1

Flexural strength followed almost the same pattern as obtained in compressive strength in that, at increased temperature (Table 3 and Figure 8), flexural strength reduced, also, due to gradual weakening of the cohesive bond between clay particles plus reduction in adhesion between particles of the WGP additives and clay particles. As WGP increased in the samples, the value of ΔF% (where ΔF% denotes percentage reduction in flexural strength from one temperature to the next) reduced, due to the effect of increased strength of adhesion between particles as WGP increased in the samples.

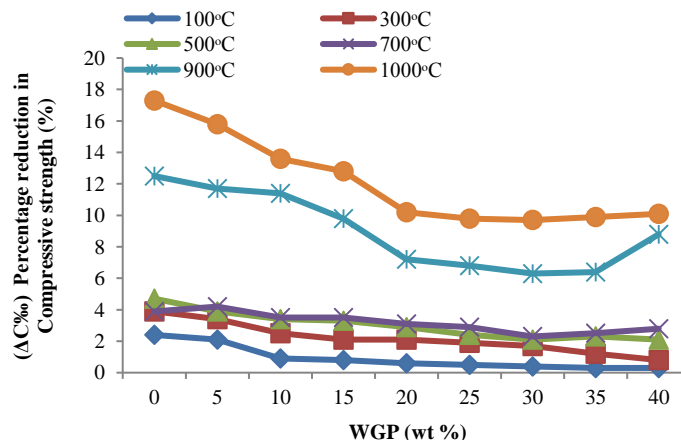


Fig. 8 Percentage reduction in flexural strength at increased temperature

Going from 100 °C to 700 °C for 0 to 50 wt. % WGP, percentage reduction in flexural strength ΔF% increased gradually, for each WGP content, ranging from 2.4 % to 3.9 % for 0 wt. % WGP, 2.1 to 4.2 % for 5 wt. % WGP, 0.9 to 3.5 % for 10 wt. % WGP, 0.8 to 3.5 % for 15 wt. % WGP, 0.6 to 3.1 % for 20 wt. % WGP, 0.5 to 2.9 % for 25 wt. % WGP, 0.4 to 2.3 % for 30 wt. % WGP, 0.3 to 2.5 % for 35 wt. % WGP and 0.3 to 2.8 % for 40 wt. % WGP. It was observed that at 100 °C, ΔF% value remained constant at 35 and 40 wt. % WGP content of 0.3 %. At each temperature of 100 to 700 °C, ΔF% value reduced as WGP content increased. From 700 to 900 °C for each sample, ΔF% value also reduced drastically just like in the case of ΔC% for compressive strength. The value (700 to 900 °C) was from 3.9 to 12.5 % for 0 wt. % WGP, 4.2 to 11.7 % for 5 wt. % WGP, 3.5 % to 11.4 % for 10 wt. % WGP, 3.5 to 9.8 % for 15 wt. % WGP, 3.1 to 7.2 % for 20 wt. % WGP, 2.9 to 6.8 % for 25 wt. % WGP, 2.3 to 6.3 % for 30 wt. % WGP, 2.5 to 6.4 % for 35 wt. % WGP and 2.8 to 8.8 % for 40 wt. % WGP. At 1000 °C, ΔF% further fell to 17.3 %, 15.8 %, 13.6 %, 12.8 %, 10.2 %, 9.8 %, 9.7 %, 9.9 % and 10.1 % for 0, 5, 10, 15, 20, 25, 30, 35 and 40 WGP content respectively. The high increase in value was attributed to the fact that at temperature up to 900 °C, there was drastic weakening of the bond and degradation of the glass phase present. This further confirms that, the working temperature of ceramic samples in this study is less than ≤ 700 °C.

c. Evaluation of flexural strain at different temperature

Table 4 Flexural strain at different temperatures

% WGP content in samples	Flexural strain at 26-29 °C	Flexural strain (at fracture) at different temperatures (α) °C					
		100 °C	300 °C	500 °C	700 °C	900 °C	1000 °C
0	0.0110	0.0113	0.0125	0.0137	0.0158	0.0213	0.0286
5	0.0081	0.0115	0.0121	0.0137	0.0149	0.0204	0.0256
10	0.0063	0.0111	0.0146	0.0131	0.0132	0.0195	0.0234
15	0.0041	0.0101	0.0118	0.0118	0.0122	0.0142	0.0196
20	0.0033	0.0087	0.0098	0.0097	0.0117	0.0118	0.0178
25	0.0018	0.0056	0.0098	0.0056	0.0099	0.0103	0.0165
30	0.0009	0.0056	0.0099	0.0023	0.0096	0.0089	0.0146
35	0.0006	0.0078	0.0087	0.0014	0.0056	0.0076	0.0139
40	0.0004	0.0106	0.0086	0.0011	0.0034	0.0053	0.0133

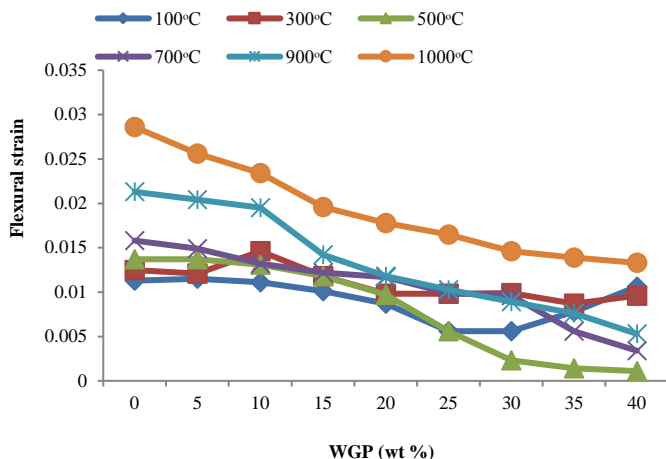


Fig. 9 Effects of increased temperature on flexural strain

Flexural strain was observed to increase at increased temperature (Table 4 and Figure 9), while flexural strength reduced with increased temperature as a result of the weakening of the bond and easier flow of the particles, aided by thermal stress. At room temperature, flexural strain reduced with increased WGP proportion in samples. At 100 °C, the value reduced from 0 wt. % to 30 wt. % additive after which there was increase in the value at 35 – 40 wt. % due to increased flow which was attributed to increased thermal energy of particles. At 300 °C, strain reduced from 0 wt. % of additive, peaked at 10 wt. % additive and further reduced as WGP proportion increased. At 500 to 1000 °C, there was reduction in strain as WGP increased from 0 wt. %. Going from 100 to 1000 °C, for each mix proportion, strain was observed to increase due to increased flow.

d. Effects of increased temperature on impact resistance

Table 5 Number of cycle to failure at different temperatures

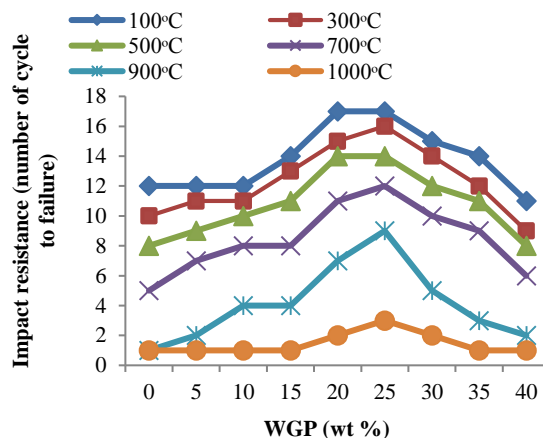
% WGP content in samples	Number of cycle to failure at 26 °C	Impact resistance (number of cycle to failure)						
		100 °C	300 °C	500 °C	700 °C	900 °C	1000 °C	
0	12	12	10	8	5	1	1	
5	12	12	11	9	7	2	1	
10	13	12	11	10	8	4	1	
15	15	14	13	11	8	4	1	
20	17	17	15	14	11	7	2	
25	18	17	16	14	12	9	3	
30	16	15	14	12	10	5	2	
35	14	14	12	11	9	3	1	
40	12	12	10	8	5	1	1	

Impact resistance was evaluated by number of cycle to failure for samples at different temperatures. The value at room temperature (26 °C) increased as WGP amount increased up to 25 wt. % before declining at 30 wt. % (Table 5 and figure 10). The resistance to impact was due to closeness of particles and strength of bond between particles. At 30 wt. % the brittle nature of the glassy phase had a toll on impact resistance which explains reduction in the number of cycles to failure from 30 to 40 wt. %.

At increased temperature, the instability of the particles due to increased excitation resulted in increased kinetic energies of particle and led to lower compactment of particles. This led to lower adhesion between clay and glass particles, thereby causing reduction in resistance to impact.

At 100 °C, impact resistance for all samples remained almost constant due to lower stress level induced in the samples. As temperature increased, from 300 to 1000 °C, residual stress increased in the samples resulting in further reduction in Figure 10: Effects of increased temperature on impact resistance.

impact resistance evaluated by number of cycles to fracture. At 700 to 900 to 1000 °C, the impact resistance depreciated greatly, owing to increased residual



stress and instability of particles as a result of thermal excitation. From 26 °C to 300 °C, difference in number of cycle to failure for all samples was in the range of 1 to 2 which explains a relative stability in impact resistance at those temperatures for all samples. At application which requires impact, temperature should be ≤ 300 °C.

e. Linear and volumetric thermal expansion at different temperatures

Table 6 Variation in Linear thermal expansion at different temperature

% WGP content in samples	Linear thermal expansion at different temperature					
	100 °C (x10 ⁻⁵ /K)	300 °C (x10 ⁻⁵ /K)	500 °C (x10 ⁻⁵ /K)	700 °C (x10 ⁻⁵ /K)	900 °C (x10 ⁻⁵ /K)	1000 °C (x10 ⁻⁵ /K)
0	0	0.97	3.92	5.27	8.28	12.37
5	0	0.88	3.34	5.05	7.45	12.04
10	0	0	2.77	4.79	7.74	11.45
15	0	0	2.42	4.54	6.73	11.13
20	0	0	2.19	4.13	6.45	7.12
25	0	0	1.83	1.84	3.13	6.43
30	0	-1.24	1.14	1.75	3.79	8.43
35	0	-0.89	2.71	2.63	8.24	7.34
40	0	-0.15	2.71	2.14	8.24	6.32

Increase in thermal conductivity on the other hand brought about lowering of thermal expansivity since particles are bonded strongly. Thermal expansivity reduced with increasing WGP proportion leading to strong adhesion between clay and WGP particles. The results for thermal expansivity agrees with [4] which also recorded reduction in thermal expansion coefficient as egg shell content increased in fired clay but contrary to result obtained in [6], whereby thermal conductivity reduced with increased content of additive. In this study and in [4], porosity reduced with increased additive while in [6] porosity increased with increased additive which explained the difference in that, with reduced porosity, thermal conductivity increased, and vice versa, in the case of increased porosity with increased proportion of additives. Linear and volumetric thermal expansivity were evaluated at different temperatures of 100 to 1000 °C by measuring change in dimension at those temperatures. It was observed that at higher temperature, linear expansivity increased (Table 6 and Figure 11) owing to weaker bond within particles, which led to increase in interparticle distance, hence resulting in higher degree of expansion.

For 100 °C, there was no linear expansivity indicating dimensional stability at that temperature because of the fact that the thermal stress exposure was not enough to cause substantial weakening of the bond between particles. At 300 °C, the linear expansion only occurred at 0 and 5 wt. % of WGP while there was contraction for samples containing 30 to 40 wt. % WGP proportion. For samples containing 10 to 25 wt. %, there was 0 values for expansion due to thermal stability at that temperature. This indicates that the thermal stress was only enough to cause vibration of the particles about their mean position, without any dissociation of the bond, even though the strength of the bond reduced which was

explained by lower reduction in compressive and flexural strength at this temperature (Table 2 and 3). It was further observed that at temperature (300 to 500 °C), linear thermal expansivity reduced from 0 to 30 wt. % owing to the strong bond and lower heat capacity of the glassy phase at such temperature, but at 35 and 40 wt. %, the value increased indicating weakening of the bond. Increment in expansivity value from 500 to 700 °C was 57 % from 5.27 to $8.28 \times 10^{-5}/K$ for 0 wt. %, 47.5 % from 5.05 to $7.45 \times 10^{-5}/K$ for 5 wt. %, 61.6 % from 4.79 to $7.74 \times 10^{-5}/K$ for 10 wt. %, 48.2 % from 4.54 to $6.73 \times 10^{-5}/K$ for 15 wt. %, 56.2 % from 4.13 to $6.45 \times 10^{-5}/K$ for 20 wt. %, 70 % from 1.84 to $3.13 \times 10^{-5}/K$ for 25 wt. %, 116.6 % from 1.75 to $3.79 \times 10^{-5}/K$ for 30 wt. %, 213 % from 2.63 to $8.24 \times 10^{-5}/K$ for 35 wt. % and 285 % from 2.14 to $8.24 \times 10^{-5}/K$ for 40 wt. %.

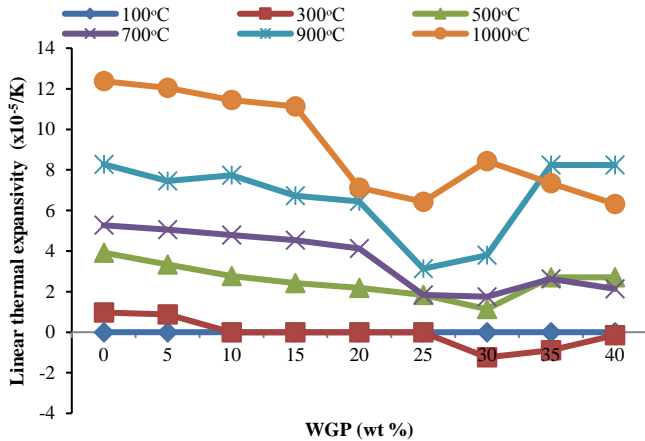


Fig. 11 Effects of WGP on linear thermal expansion at different temperatures

From this percentage increase, it was noted that as WGP content increased, the percentage rise in expansivity increased, indicating high level of degradation of the glassy phase and weakening of the bond between particles. This still further confirms that the working temperature of the set of ceramic samples analyzed in this study should not be greater than 700 °C. Percentage increase in expansivity increased at 1000 °C at 49 %, 62 %, 48 %, 65 %, 63 %, 127 %, 70 %, for 0 to 30 wt. % additions. This can be attributed to the further degradation of the glassy phase and weakened adhesion between the clay and WGP. In the case of 35 and 40 wt. % WGP, expansivity reduced from 8.24 for both, to 7.34 and $6.32 \times 10^{-5}/K$ respectively due to slight contraction.

Table 7 Variation in Volumetric thermal expansion at different temperature

%WGP content in samples	Volumetric thermal expansion at different temperature					
	100 °C (x10 ⁻⁵ /K)	300 °C (x10 ⁻⁵ /K)	500 °C (x10 ⁻⁵ /K)	700 °C (x10 ⁻⁵ /K)	900 °C (x10 ⁻⁵ /K)	1000 °C (x10 ⁻⁵ /K)
0	0	0.262	0.273	0.345	0.412	0.852
5	0	0.215	0.258	0.322	0.378	0.794
10	0	0	0.229	0.305	0.354	0.772
15	0	0	0.194	0.215	0.322	0.764
20	0	0	0.183	0.217	0.294	0.621
25	0	0	0.164	0.217	0.293	0.574
30	0	-0.184	0.154	0.158	0.214	0.525
35	0	-0.172	0.132	0.149	0.233	0.574
40	0	-0.198	-0.121	0.137	0.199	0.599

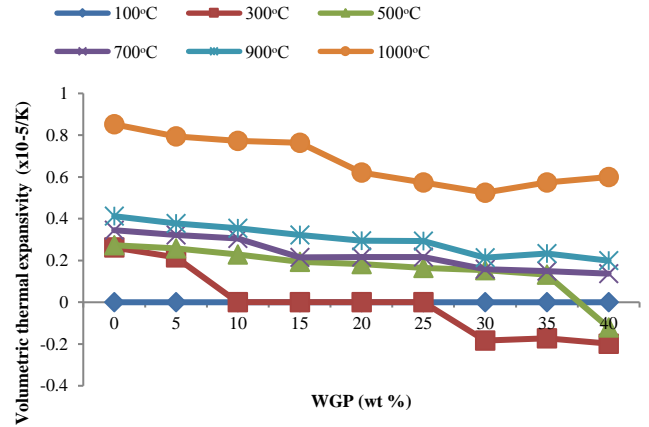


Fig. 12 Effects of WGP on volumetric thermal expansion at different temperatures

Volumetric thermal expansivity was evaluated by measuring increment in the dimension of the rectangular prism sample. This property follows the same trend as in the case of linear expansion with the same reason at each temperature. With increased temperature, the value increased and with increasing WGP content, the trend reduced down the line.

Thermal shock resistance and cooling rate

a. Experimental results on thermal shock resistance

Effects of WGP on thermal shock resistance were measured using 3 ways of experimenting:

Table 8 Number of cycle at which crack appeared for Exp. 1, 2 and 3

WGP	0	5	10	15	20	25	30	35	40
Number of cycles in Exp. 1	21	22	23	15	14	16	16	10	10
Number of cycles in Exp. 2	65	62	60	60	43	36	34	29	21
Number of cycles in Exp. 3	44	44	45	43	38	36	34	22	19

Figure 13 shows the number of cycles for each case. For case Exp. 1, the number of cycles after samples was exposed to 1000 °C increased from 21 to 23 for 0 wt. % to 10 wt. % of WGP, at further increased amount of WGP, the value reduced to 15 at 15 wt. % content remained constant until it fell at 35 wt. % of the additive. Going by [26], WGP content should not be more than 10 % in bricks for refractory. For Exp. 2, shock resistance based on number of cycles recorded decreased from 65 cycles to 21 cycles from 0 to 40 wt. % of WGP. This is due to the brittle nature of the glass phase formed and can be deduced that increased proportion of WGP particles resulted in lower thermal shock resistance of bricks exposed to air cooling. For Exp. 3, water was employed as a means of cooling; the shock resistance measured by number of cycles, reduced from 0 wt. % WGP content to 40 wt. % WGP content. Therefore, thermal shock resistance in the samples reduced as WGP content increased. In environment whereby cooling is done by combine action of air and water, ≤15 wt. % WGP addition to bricks might suffice in clay materials, since from 0 to 15 wt. % difference in the number of cycles for Exp. 1, 2 and 3 was in the range of 2 to 5 cycles.

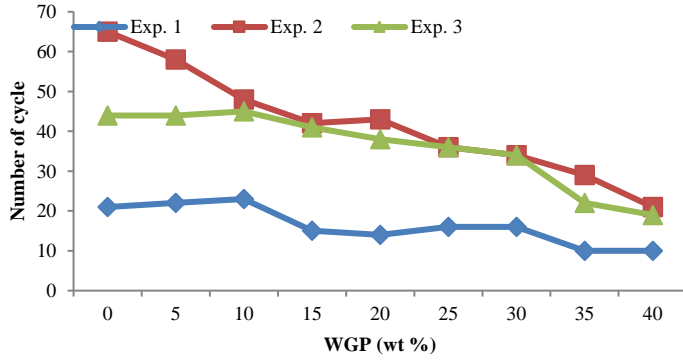


Fig. 13 Effect of WGP content on thermal fatigue

b. Cooling rate

i. Normalized cooling

It was observed that with increasing WGP content, cooling rate increased (Figure 14) with WGP addition, due to enhanced thermal conductivity. Highest cooling rate was recorded at 40 wt. % for each of the temperatures considered. Therefore, in applications whereby normal cooling rate is employed, increased WGP content in fired bricks is recommended.

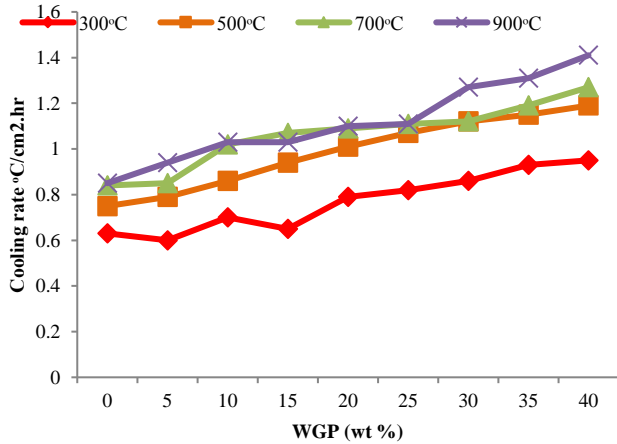


Fig. 14 Effect of WGP content on cooling rate

ii. Rapid cooling (Fast cooling rate per cross section)

Figure 15, shows the effects of WGP on cooling rate of samples at fast cooling rate using water. The incorporation of WGP into bricks at increasing weight content resulted into higher cooling rate due to high emissivity at elevated temperatures. At high temperature, particles are highly excited leading to mobility and increased interparticle spacing. The process of rapid cooling results into forceful dissipation of already absorbed energy in solid bodies, causing inherent particles to maintain disoriented positions at low temperature as the heat is being dissipated. This caused distortion in the arrangement and orientation of particles which resulted in increased brittleness in the samples. Furthermore, at high temperature of 900 °C where degradation of glassy phase was more pronounced, as cooling rate became high, the glassy phase were not allowed to re-form causing uneven distribution of glass particles within the clay matrix as shown in Figure 18. This initiates high level of brittleness because of high strain energy induced around the unevenly distributed glass particles, resulting in low strength as expressed in Figure 18.

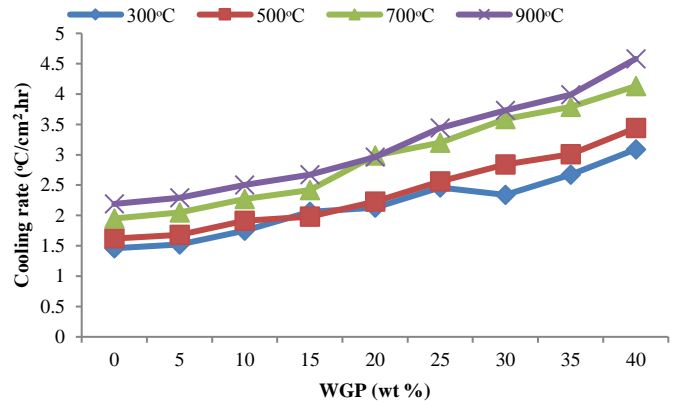


Fig. 15 Effect of WGP on High cooling rate per cross section of samples

iii. Cooling rate coefficient

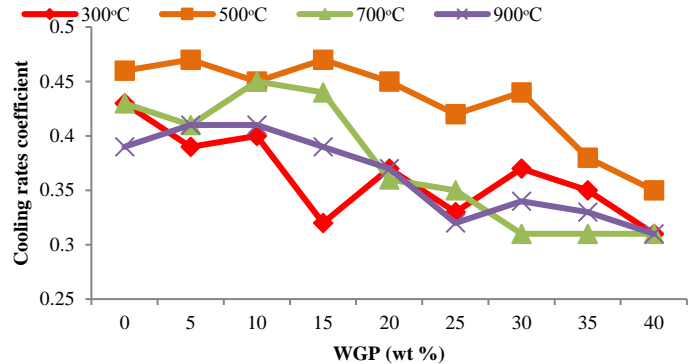


Fig. 16 Cooling rate coefficient with increasing WGP

Figure 16 shows the coefficient of cooling rate at different temperature with increasing WGP content. The cooling rate at 500 °C is the highest indication that normalized cooling rate for all samples is more effective than fast cooling at that temperature. Highest cooling rate coefficient for all samples was recorded at 500 °C for 15 wt. % WGP, indicating that for applications which may involve normalized cooling and fast cooling, temperature should not exceed 500 °C for all composition. Therefore, WGP composition of 15 wt. % gave the optimum value.

Morphological behaviour: effect of fast cooling on strength performance of clay sample

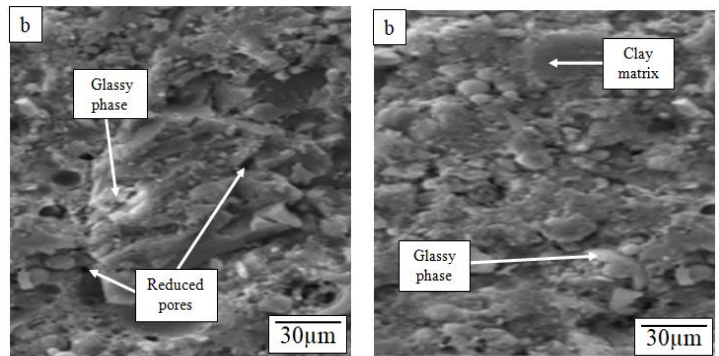


Fig. 17 Surface image of sample with 30 wt. % WGP (a) and 35 wt. % WGP (b), before rapid cooling.

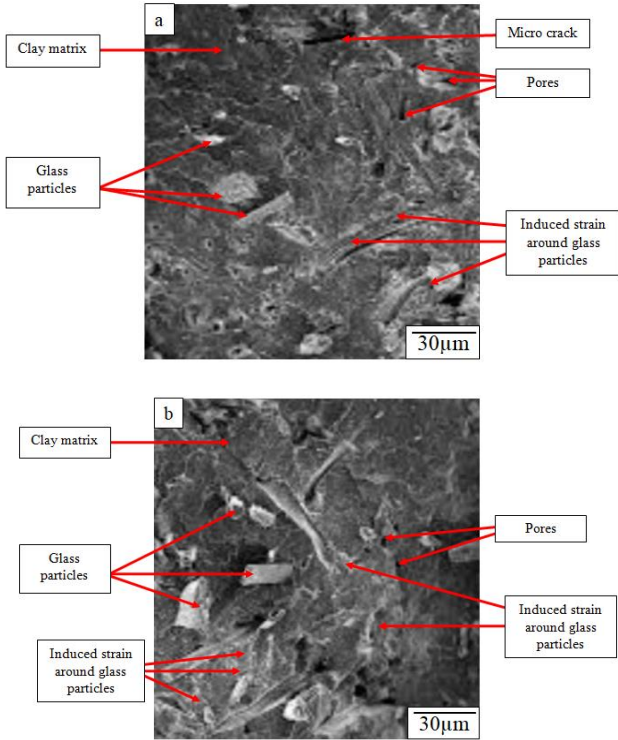


Fig. 18 Surface image of sample with 30 wt. % WGP (a) and 35 wt. % WGP (b), cooled rapidly from 900 °C to room temperature

Table 9 Impact resistance (number of cycle to failure) after fast cooling

% WGP content in samples	Number of cycle to failure at 26 °C	Impact resistance (number of cycle to failure) of samples after fast cooling			
		300 °C	500 °C	700 °C	900 °C
20	18	7	5	2	1
25	16	8	6	2	1
30	16	7	6	2	1
35	14	5	3	1	1
40	12	5	3	1	1

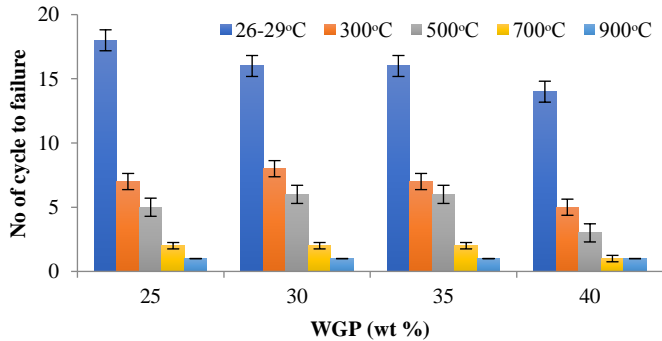


Fig. 19 Impact resistance (number of cycle to failure) of samples at room temperature (26-29 °C) and those fast cooled to room temperature from 300, 500, 700 and 900 °C

Impact resistance of samples after brick samples were fast cooled from high temperature reduced when compared to impact resistance of samples that were not fast cooled. For 20 wt. % WGP, the number reduced from 18 cycles to 7, 5,

2, 1 when fast cooled from 300, 500, 700 and 900 °C respectively, as indicated in Table 9, which indicates that fast cooling of brick samples from high temperature enhances brittleness or ease to fracture in samples. For 25 wt. % WGP, the number reduced from 16 cycles for sample tested at room temperature to 8, 6, 2 and 1 cycles for samples fast cooled from 300, 500, 700 and 900 °C respectively. In the case of 30, 35 and 40 wt. % WGP fast cooled, number of cycle to failure was 7, 6, 2, and 1 for 30 wt. % WGP, 5, 3, 1, 1 for 35 wt. % WGP and 5, 3, 1, 1 for 40 wt. % WGP (Table 9). From the results, it is clear that fast cooling reduces resistance to impact (Figure 19).



Fig. 20 Image showing crack path on surface of bricks during test

Comparing compressive strength of samples tested at room temperature and those tested after rapid cooling, it was observed that there was great reduction in strength. At fast cooling rate, particles are disarranged and disoriented leading to high strain energy stored in samples which aids ease to fracture in samples. The effect was more pronounced as temperature increased from 300 to 500 to 700 to 900 °C. Respective reduction in strength while comparing values at 26-29 °C to 300, 500, 700 and 900 °C was 45 %, 50 %, 80 % and 89 % for 25 wt. % WGP, 46 %, 50 %, 84 % and 88 % for 30 wt. % WGP, that of 35 wt. % WGP was 53 %, 60 %, 83 %, and 88 %. For 40 wt. % WGP, the reduction was 54 %, 64 %, 82 % and 90 % respectively (Figure 21).

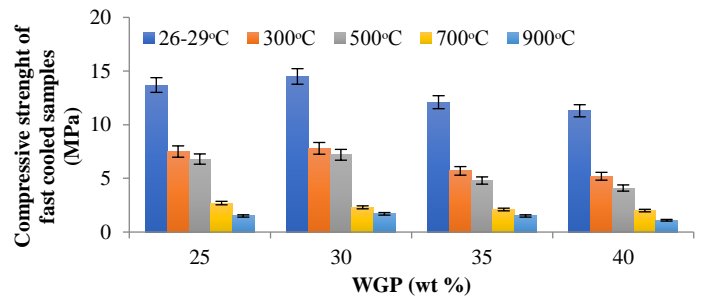


Fig. 21 Comparison of compressive strength of samples at room temperature (26-29 °C) and those fast cooled to room temperature from 300, 500, 700 and 900 °C

For flexural strength (figure 22), respective reduction in strength while evaluating from 26-29 °C to 300, 500, 700 and 900 °C was 52 %, 54 %, 93 % and 99 % for 25 wt. % WGP, 52 %, 53 %, 91 % and 98 % for 30 wt. % WGP, that of 35 wt. % WGP was 53 %, 50 %, 81 % and 99 % and for 40 wt. % WGP, the reduction was 51 %, 53 %, 94 % and 99 % respectively. Analyzing the percentage reduction for compressive strength, the effect was more pronounced at temperatures of 700 and 900 °C with reduction varying from 80 to 84 % for 700 °C and 88 to 90 for 900 °C. In the case of flexural strength, the reduction was also more pronounced at temperatures of 700 and 900 °C varying from 81 to 95 % for 700 °C and 98 to 99 for 900 °C for samples containing 25 to 40 wt. % of WGP. The effect had higher toll on flexural than compressive strength and at 900 °C, highest percentage reduction was recorded in flexural strength.

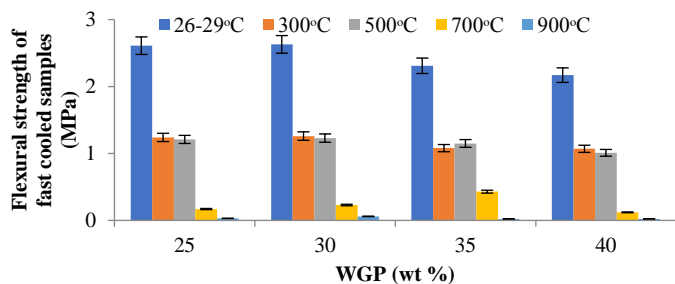


Fig. 22 Comparison of flexural strength of samples at room temperature (26-29 °C) and those fast cooled to room temperature from 300, 500, 700 and 900 °C

CONCLUSIONS

Effects of elevated temperature and waste glass powder (WGP) content on thermo-mechanical properties of fired ceramic products were examined in this study and response of samples to different temperatures were analyzed. From the results obtained, the following conclusion were made

- With increased temperature from 26-29 °C to 700 °C, mechanical performance tends to reduce gradually due to gradual weakening of bond and degradation of the glassy phase present in the samples
- At up to 900 °C the performance reduced drastically due to high extent of bond weakening and fastened degradation of the glassy phase coupled with increased thermally induced residual stress and high excitation of particles/atoms, hereby, dictating an operating temperature of ≤ 700 °C for samples.
- Thermal conductivity, diffusivity and emissivity increased with increasing WGP content while thermal expansivity and specific heat capacity reduced as percentage WGP increased in the samples
- For samples heated to 1000 °C, thermal shock resistance improved from 0 to 10 wt. % WGP while at further addition of WGP, the resistance reduced, in this case refractory bricks, WGP should not exceed 10 wt. %.
- Thermal shock resistance remains stable in samples at WGP content of ≤ 15 wt. %, beyond this, there was reduction (for samples air/water cooled from 300 °C). Therefore, for ceramic products to be exposed to operating temperature of ≤ 300 °C, WGP should be ≤ 15 wt. %.
- Higher thermal conductivity and lower specific heat capacity resulted into increased cooling rate at higher WGP addition, hence for fast cooling rate applications, increased proportion of WGP (between 5 to 40 wt. %) may be recommended, however for applications whereby compressive and flexural strength are important as well as increased cooling rate, WGP content of between 5 to 30 wt. % may be suitable, since the strength reduced at 35 and 40 wt. % at room temperature, as shown in Table 2 and 3.
- The coefficient of cooling rate at 500 °C was the highest indication that normalized cooling rate for all samples is more efficient than fast cooling at that temperature
- Rapid cooling for heat treated bricks reduces strength largely, hence not recommended for fired clay bricks.

Acknowledgments: Authors are grateful for the support of the Metallurgical and Materials Engineering Department, Federal University of Technology Akure, Glass and Ceramic Laboratory, Federal Polytechnic, Ado-Ekiti and Landmark University Centre for Research, Innovation, and Development (LUCRID) through SDGs 9 Group Innovation, Industry and Infrastructure.

REFERENCES

1. R. Bermejo, R. Danzer: Mechanical Characterization of Ceramics: Designing with Brittle Materials, *Comprehensive Hard Materials*, 2, 2014, 285-298, <https://doi.org/10.1016/B978-0-08-096527-7.00028-3>
2. F.O. Aramide, O.D. Adepoju, A.A. Adediran, A.P.I. Popoola: Studies on the combined effects of titania and silicon carbide on the phase developments and properties of carbon-clay based ceramic composite. *Cogent Engineering*, 6, 2019, 1584938, <https://doi.org/10.1080/23311916.2019.1584938>
3. A. Shakir, A. Mohammed: Manufacturing of Bricks in the Past, in the Present and in the Future: A state of the Art Review, *International Journal of advances in applied Science*, 2(3), 2013, 145-156, <https://doi.org/10.11591/ijaas.v2i3.1751>
4. N. Tangboriboon, W. Pannangpetch, K. Aranyik, K. Petcharoen, A. Sirivat: Embedded Eggshells as a Bio-Filler in Natural Rubber for Thermal Insulation Composite Foams, *Progress in Rubber Plastics Recycling Technology*, 31, 2015, 189-206, <https://doi.org/10.1177/147776061503100304>
5. E. Bwayo, K. Obwoya Sam: Coefficient of Thermal Diffusivity of Insulation Brick Developed from Sawdust and Clays. *Journal of Ceramics*, 2014, 1-6, <https://doi.org/10.1155/2014/861726>
6. S. Ahmad, Y. Iqbal, R. Muhammad: Effects of Coal and Wheat Husk Additives on the Physical, Thermal and Mechanical Properties of Clay Bricks, *Boletin de la Sociedad Espanola de Ceramica y Vifrio*, 56(3), 2017, 131-138, <https://doi.org/10.1016/j.bsecv.2017.02.001>
7. ASTM C 1314-18: Standard Test Methods for Compressive Strength of Masonry Prisms, *ASTM International*, West Conshohocken, PA, 2018.
8. ASTM 293/C293M: Standard Test Methods for Flexural Strength of Masonry bricks (Using Simple Beam with Centre-Point Loading), *ASTM International*, West Conshohocken, PA, 2016
9. ASTM E1225-13: Standard Test Method for Thermal Conductivity of Solids Using Guarded-Comparative-Longitudinal Heat Flow Technique. *ASTM International*, West Conshohocken, PA, 2013
10. ISO 17139:2014(en): Thermophysical Properties of Ceramic Composites-Determination of Thermal Expansion. International Standard Organization, 2014.
11. ASTM E1269-11: Standard Test Method for Determining Specific Heat Capacity by Differential Scanning Calorimetry. *ASTM International*, West Conshohocken, PA, 2018
12. ASTM C1470-20: Standard Guide for Testing the Thermal Properties of Advanced Ceramics. *ASTM International*, West Conshohocken, PA, 2020.
13. ASTM E2585-09: Standard Practice for Thermal Diffusivity by the Flash Method. *ASTM International*, West Conshohocken, PA, 2009
14. ASTM C1525-18: Standard Test Method for Determination of Thermal Shock Resistance for Advanced Ceramics by Water Quenching. *ASTM International*, West Conshohocken, PA, 2018
15. J. Y. Hwang, X. Huang, A. Garkida: Waste Colored Glasses as Sintering aid in Ceramic Tile Production. *Journal of Minerals and Materials Characterization and Engineering*, 5(2), 2006, 119-129, <https://doi.org/10.4236/jmmce.2006.52008>
16. M. Abuh, C. A. Agulanna, P. E. Chimezie, J. U. Bethel-Wali: Implications and Characteristics of Waste Glass Cullet-Kaolinite Clay Ceramic. *Journal of Applied Science and Environmental Science*, 23, 2019, 513-518, <https://doi.org/10.4314/jasem.v23i3.22>
17. P. Praveen, E. Chandrasekaran, G. Viruthagiri: The effect of temperature on ceramic bricks with replacing waste glass in low volume ratio. *International Journal of Advanced Science and Research*, 3(2), 2018, 79-86
18. Chao-Wei Tang: Properties of Fired Bricks by Incorporation TFT-LCD Waste Glass Powder with Reservoir Sediments. *Sustainability*, 10 (7), 2018, 2503. <https://doi.org/10.20944/preprints201806.0229.v1>
19. H. H. Abdeen, S. M. Shihada: Properties of fired clay bricks mixed with waste glass. *Journal of Scientific Research and Reports*, 13(4), 2017, 1-9. <https://doi.org/10.9734/jsrr/2017/32174>
20. I. Demir: Reuse of waste glass in building brick production. *International Journal of Waste Management and Research*, 27, 2009, 572-577. <https://doi.org/10.1177/0734242x08096528>
21. V. Ducman, T. Kopar: Sawdust and paper-making sludge as pore-forming agents for lightweight clay bricks. *Journal of Industrial Ceramics*, 21, 2001, 81-86
22. M. E. Borredon, E. Vedrenne, G. Vilarem: Development of Eco-Friendly Porous Fired Clay Bricks using Pore Forming Agents: A Review. *Journal of Environmental Management*, 143, 2014, 186-196. <https://doi.org/10.1016/j.jenvman.2014.05.006>
23. A. Salazar: On Thermal Diffusivity. *European Journal of Physics*, 24, 2003, 351-358, <https://doi.org/10.1088/0143-0807/24/4/353>
24. Y. Zhang, Q. Li, H. Zhou: Theory and Calculation of Heat Transfer in Furnaces, *Emission and Absorption of Thermal Radiation*, 2016, 45-75,

https://www.researchgate.net/publication/304108475_Emission_and_Absorption_of_Thermal_Radiation

25. K. Radmanovic, I. Dukicand, S. Pervan: Specific Heat Capacity of Wood. *Drvna Industrija*, 65, 2014, 151-157, <https://doi.org/10.5552/drind.2014.1333>
26. Y. Shuaib-Babata, S. Yaru, S. Abdulkareem, Y. Busari, I. Ambali, S. Kabiru, Ajao, G. Mohammed: Characterization of Baruten Local Government Area of Kwara State (Nigeria) Fireclays as Suitable Refractory Materials. *Nigerian Journal of Technology*, 37, 2018, 374-386, <https://doi.org/10.4314/njt.v37i2.12>